Dissipative devices for earthquake resistant composite steel structures: bolted versus welded solution

Marco Valente[1] · **Carlo A. Castiglioni**[1] · **Alper Kanyilmaz**[1]

Abstract This paper investigates and compares the seismic performance of two types of innovative repairable fuse devices for earthquake resistant composite steel frames through experimental tests and numerical analyses. The fuses are energy dissipating devices consisting of steel plates that can be welded or bolted to the beam web and bottom flange. The numerical analyses performed in this study are based on the results of experimental tests carried out on beam-to-column sub-assemblages equipped with both the types of fuse devices. The main differences in terms of hysteretic behavior and failure modes of the fuses are identified through the experimental campaign. Detailed three-dimensional finite element models of the beam-to-column sub-assemblages are then created to provide a deeper insight into both the response and the effectiveness of the two investigated devices. On the basis of the results of both the experimental tests and numerical analyses, simplified models of different types of fuses are developed in order to study the effects of bolted and welded devices on the seismic response of composite steel frames. The results are then extended to the case of three-dimensional building structures with different number of storeys. The experimental and numerical investigations prove the effectiveness of the fuses and highlight the main differences between the two possible solutions.

Keywords Welded · Bolted · Fuse device · Energy dissipation · Numerical model · Non-linear dynamic analysis

✉ Marco Valente
marco.valente@polimi.it

[1] Department of Architecture, Built Environment and Construction Engineering ABC, Politecnico di Milano, Piazza Leonardo da Vinci 32, 20133 Milan, Italy

This is a post-peer-review, pre-copyedit version of an article published in Bullettin of Earthquake Engineering, 2016, 14, 3613-3639. The final authenticated version is available online at: http://dx.doi.org/10.1007%2Fs10518-016-0002-9

1 Introduction

Most of the structures designed according to current code procedures may experience inelastic deformations in critical regions of the main structural members under strong earthquakes (Elghazouli 2010). These inelastic deformations often result in difficult-to-repair damage, high repair costs and long disruption of occupancy or use.

Different strategies can be employed in order to reduce damage to structures under moderate to strong earthquakes (Soong and Spencer 2002). Some solutions rely on supplemental damping provided to the structure through various devices based on viscous, friction or yielding dampers. Passive damping systems can improve the seismic performance of buildings by reducing drift and inelastic deformation demands on the members of the primary lateral load resisting system.

An alternative seismic design strategy can be efficiently employed to withstand earthquake loads. It concentrates damage in removable steel yielding plates and protects the other irreplaceable parts of the structural system from yielding. The easy replacement of the dissipative elements damaged under moderate to strong earthquakes and the reduction of the repair costs are the main advantages of such a design approach (Mansour et al. 2011;Shenetal.2011).

The work described in this paper is developed within the European research program "Fuseis" (Calado et al. 2013a, b; Castiglioni et al. 2012; Danai et al. 2015), and focuses on the seismic performance of innovative composite steel frames that aim at reducing structural damage by concentrating plastic deformations in removable or repairable fuses. The fuses are energy dissipating devices that are made by introducing a discontinuity on the composite beams of a moment resisting steel frame and assembling the two parts of the beam through steel plates attached to the beam web and flange. Inelastic deformations are constrained to the removable plates and all other irreplaceable frame members and connections are protected from damage remaining in the elastic range. Additionally, it is possible to replace the damaged removable plates with new elements.

Two different types of dissipative devices are analyzed and compared in this study. Figures 1 and 2 show schematic drawings and general views of the fuse device configuration for the welded and bolted solutions, respectively. The device consists of steel plates that can be welded or bolted to the web and bottom flange of the beam with a specifically detailed gap in the concrete slab. The gap in the slab is intended to prevent damage to the concrete, allowing for large plastic rotations in the fuse without contact between the two parts of the concrete slab. The width of the gap in the concrete slab may be smaller than that of the two steel parts of the fuse: there are no strict indications, but the recommended value is about 10 %of the height of the slab. The width of the gap between the two steel parts of the fuse can be assumed equal to about 10 % of the overall height of the composite cross-section. It is

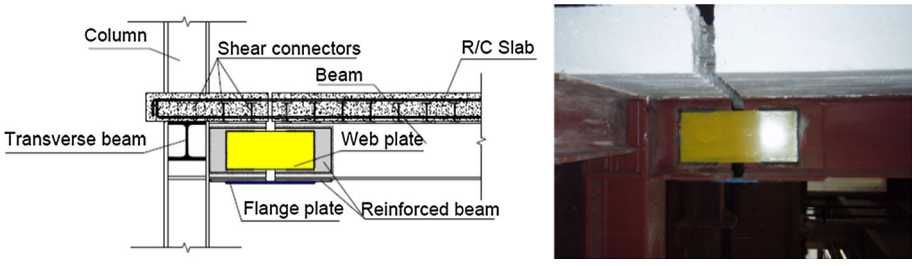

Fig. 1 Fuse device configuration for the welded solution: schematic drawing and general view of a beam-to-column sub-assemblage with welded fuse device used in the experimental tests

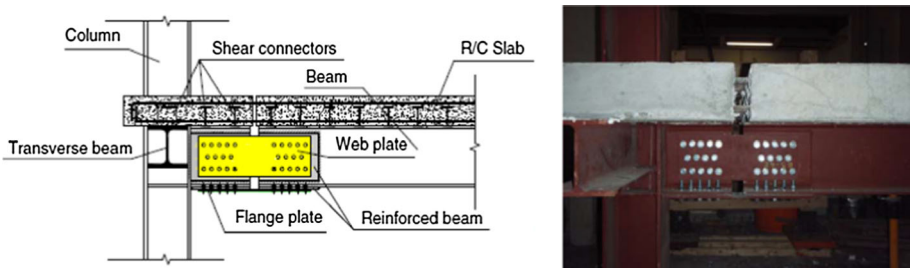

Fig. 2 Fuse device configuration for the bolted solution: schematic drawing and general view of a beam-to-column sub-assemblage with bolted fuse device used in the experimental tests

recommended that longitudinal steel rebars of the concrete slab should be continuous over the gap in order to ensure the transmission of stresses and should be designed by forcing the plastic neutral axis to lie within the slab thickness in order to prevent their yielding. To achieve such a result, it is recommended that the overall area of the longitudinal steel rebars in the concrete slab is more than twice the cross-sectional area of the flange plate.

The main aim of this study is to investigate and compare the seismic performance of welded and bolted fuses. In particular, the following issues are addressed: (1) to identify the main characteristics of the seismic response of both the devices; (2) to assess the main effects of bolted and welded fuses on the seismic response of composite steel frames and building structures.

To this aim, the results of the experimental tests performed on beam-to-column sub-assemblages equipped with fuse devices are used to calibrate simplified numerical models of the fuses for seismic analyses of composite steel frames. Moreover, experimental tests provide useful information about the failure modes of the different fuses and about the repairability and replacement of the steel plates of the device.

Detailed three-dimensional (3D) finite element (FE) models of the beam-to-column sub-assemblages are developed to assess the effectiveness of the fuse devices to protect the main irreplaceable structural elements from damage and to obtain the main mechanical parameters for different types of fuse devices that were not tested during the experimental campaign.

Then, simplified models of the steel energy dissipating devices are developed and calibrated on the basis of existing experimental results and detailed 3D FE models. The simplified models are found able to accurately predict the hysteretic behavior of the fuses and are used to investigate the seismic performance of a steel frame and different building structures equipped with fuse devices. The seismic response of innovative structures is compared with conventional structures through non-linear dynamic and static pushover analyses. The study compares the two different typologies of fuse devices, highlighting their main characteristics and the most important effects on the seismic response of composite steel structures.

2 Experimental tests and numerical analyses on beam-to-column sub-assemblages

2.1 Experimental tests

The experimental test set-up of the laboratory tests performed at Instituto Superior Tècnico of Lisbon is shown in Fig. 3. Cyclic tests were conducted on several test specimens in

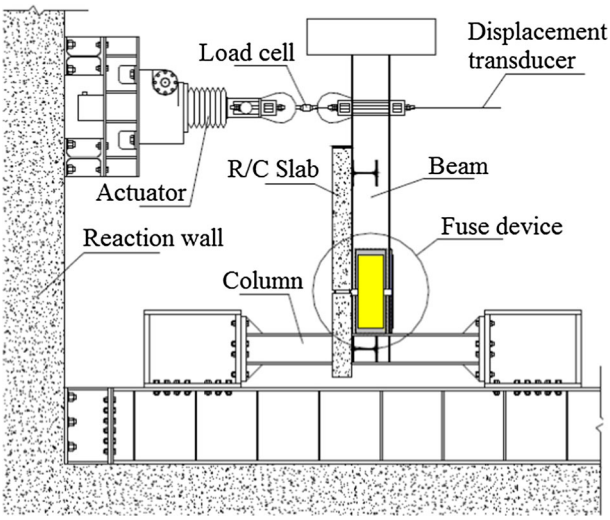

Fig. 3 Experimental test set-up of the laboratory tests performed at Instituto Superior Tècnico of Lisbon

order to assess the performance of different types of fuse devices. The test specimens were typical beam-to-column sub-assemblages, consisting of a composite beam (IPE300 profile supporting a 150 mm thick and 1450 mm wide reinforced concrete slab) and a steel column (HEB240 profile). The device is composed of steel plates that may be welded or bolted to the beam web and bottom flange with a specifically detailed gap in the concrete slab. The laboratory tests were conducted by applying cyclic variable amplitude dis-placements at the free edge of the beam of the specimens.

Experimental tests provided data for important parameters of the devices used in the present numerical study, useful to describe the response of the fuses to monotonic and cycling loading. The moment-rotation diagrams obtained from the test specimens with welded and bolted fuses are compared in Fig. 4 for the three different types of plates investigated in this study. Moreover, the experimental campaign showed that the innovative system may represent an economical solution having the following advantages: inelastic deformations are concentrated in steel plates that act as dissipative fuses and the fuses can be easily fabricated, installed and removed, limiting repair costs and time required to make the building operational after severe earthquakes. The main failure modes for the two types of fuses were identified and compared.

A comprehensive description of the results of the extensive experimental campaign carried out at Instituto Superior Tècnico of Lisbon can be found in (Calado et al. 2013a) for welded fuses and in (Calado et al. 2013b) for bolted fuses.

2.2 Three-dimensional finite element models

Detailed 3D FE models of beam-to-column sub-assemblages with fuse devices were developed by using the ABAQUS software package (Abaqus 2014) in order to reproduce the behavior of the fuse system of the specimens tested at Instituto Superior Tècnico of Lisbon, Fig. 5. Some different flange plates of the fuse devices used in the experimental tests were modeled in this study. The flange plates were characterized by different geometric and mechanical parameters, such as the geometric slenderness and the resistance capacity ratio.

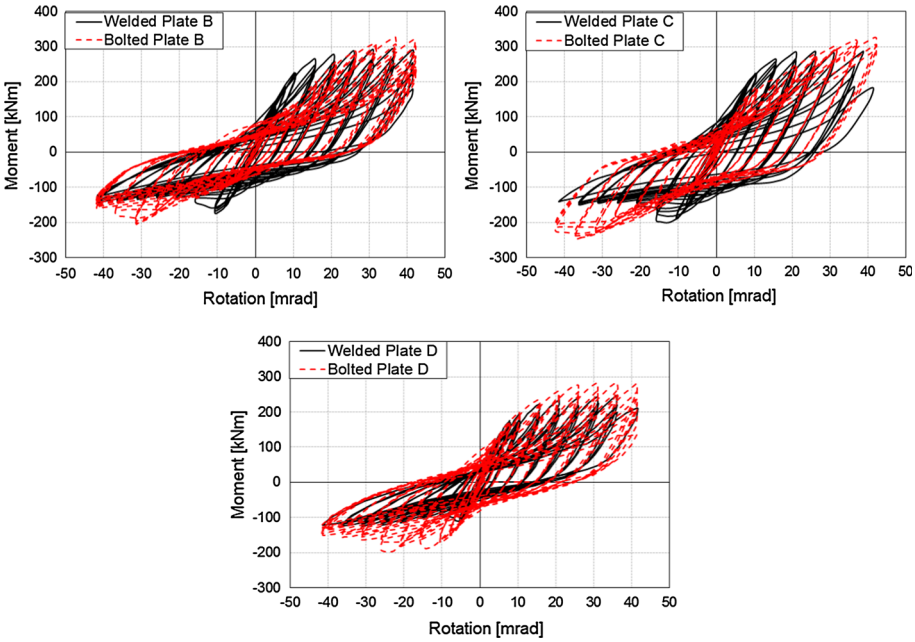

Fig. 4 Moment-rotation diagrams obtained from experimental tests: comparison between specimens with welded and bolted fuses for different plates

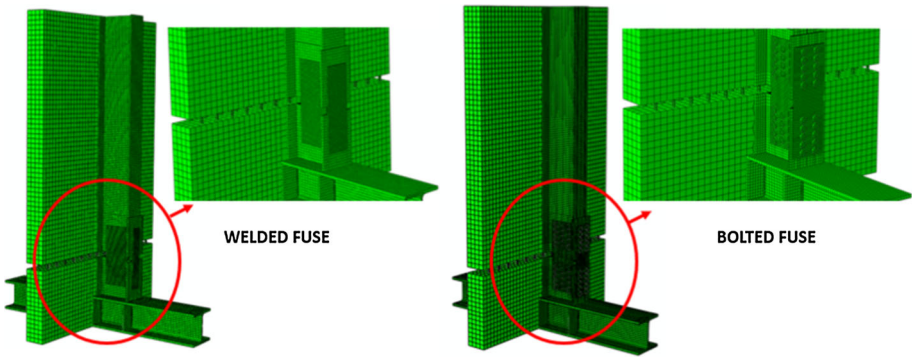

Fig. 5 Finite element models of the specimens used in the experimental tests: welded and bolted fuses

The geometric slenderness λ of the flange plate is defined as:

$$\lambda = \frac{L_0}{t_{fuse}} \tag{1}$$

where L_0 is the free buckling length of the fuse and t_{fuse} is the thickness of the fuse flange plate. For welded fuses, the free buckling length L_0 is given by the horizontal distance between the end of the lap welds on each side of the gap on the fuse section. For bolted fuses, the free buckling length L_0 is given by the horizontal distance between the innermost bolt rows of the fuses, Fig. 6. Within this length both flange and web plates are

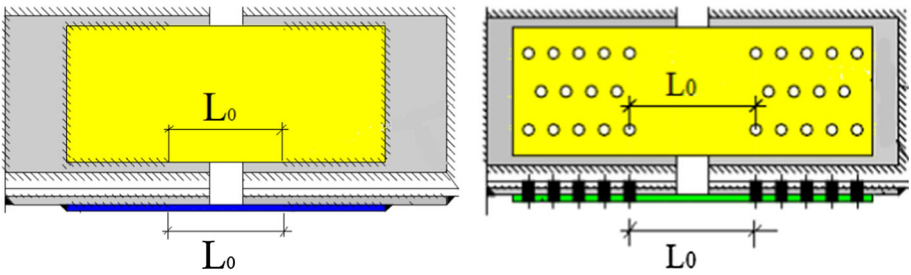

Fig. 6 Free buckling length ($L_0 = 170$ mm) of welded and bolted fuses

Table 1 Main dimensions and geometric slenderness of the welded and bolted flange plates of the different fuses

	Welded fuses			Bolted fuses		
Flange plate	B	C	D	B	C	D
Thickness (mm)	10	12	8	10	12	8
Width (mm)	130	110	100	170	150	140
Geometric slenderness	17	14.1	21.3	17	14.1	21.3

unrestrained and therefore are free to buckle. The FE models investigated in this study exhibit the same free buckling length (170 mm) of the steel plates for all the configurations of the fuses.

The resistance capacity ratio α of the fuse is defined as:

$$\alpha = \frac{M_{\max,\text{fuse}}}{M_{pl,beam}} \tag{2}$$

where $M_{max,fuse}$ is the maximum moment capacity developed by the fuse device and $M_{pl,beam}$ is the plastic resistant moment of the unreinforced area of the composite cross-section of the beam.

The dimensions (thickness and width) and the geometric slenderness of the welded and bolted flange plates of the fuses investigated in the numerical analyses are summarized in Table 1. It is worth mentioning that bolted and welded fuses are characterized by the same net cross-section.

The elements used for the development of the models are solid (continuum) elements named C3D8R, which are linear displacement interpolation solid elements with reduced integration. Reduced integration elements are chosen in order to decrease computational time, which would be excessive in the case of higher order elements. At least two elements are employed in the thickness of steel flanges and plates in order to accurately reproduce the bending behavior. The mesh is finer in the parts of the model where high stress concentrations are expected.

Shear connection between slab and beam and all other constraints are modeled by using the "tie" option (Vasdravellis et al. 2009a). Using this constraint type, the degrees of freedom (rotational and translational) between the nodes of the two surfaces which are tied to each other are constrained to maintain the same values.

In the models with welded fuses, the steel plates of the fuse device are tied to the web and bottom flange of the beam through the weld parts. In the models with bolted fuses, the fuse device is modeled by introducing contact interactions among the beam, bolts and steel plates.

Structural steel and reinforcing rebars in the slab are assumed to behave like an elastic–plastic material with hardening both in compression and in tension and the Von Mises yield criterion is used. The steel grades S275 and A500 are used, respectively, for structural elements and reinforcing rebars of the FE model representing the test specimens. In the case of bolted fuses, bolt steel is also modelled within the framework of von Mises plasticity with linear hardening, but presents much higher strength and limited ductility derived from the experimental data.

Numerical analyses and experimental tests showed that the behavior of the fuse was mainly affected by the yielding and buckling of the steel plates and no major cracking of the slab was observed. Consequently, in numerical models concrete is modeled with an elastic behavior, thus significantly reducing the high computational demand, and buckling of the flange plate is properly simulated at hogging rotation (negative bending moment and slab in tension).

In this study the FE models are analyzed in terms of deformed shape and equivalent plastic strain (PEEQ) contour plot. The equivalent plastic strain PEEQ is defined as $PEEQ = \sqrt{\frac{2}{3}\varepsilon_{ij}^{p}\varepsilon_{ij}^{p}}$ and it represents the equivalent plastic strain accumulated during the displacement-controlled loading history (Vasdravellis et al. 2009b; Giannuzzi et al. 2014).

The numerical analyses performed on the detailed 3D FE models of beam-to-column sub-assemblages provided useful information about the effectiveness of the device to concentrate plastic deformations and to protect the other irreplaceable structural elements from damage. Moreover, the detailed 3D FE models were used to obtain some mechanical characteristics (elastic stiffness and moment resistance capacity under sagging and hogging rotations) of different types of welded and bolted fuses that were not tested during the experimental campaign.

2.3 Discussion of results

The results obtained from the numerical simulations carried out through a displacement-controlled increasing (monotonic) loading history applied at the free edge of the beam are reported in this study. Figure 7 shows the deformed shape and the PEEQ contour plot for the models with welded flange plates C and D under sagging and hogging rotations (approximate device rotation = 40 mrad).

The results of the analyses under sagging moment (positive bending moment and slab in compression) show that in both the numerical models plastic deformations concentrate at the web and flange plates, ensuring that the plastic hinge occurs at the fuse section and protecting the remaining irreplaceable parts of the joint. High PEEQ values and stress concentrations are registered near the welds of the web plates and in the middle of the flange plates. This result is in agreement with the typical failure modes observed in the specimens tested in the laboratory, consisting of the development of cracks at the gross mid-section of the flange plate under tension, as shown in Fig. 8. The model with welded plate D exhibits higher PEEQ values in the fuse device than the model with welded plate C.

The results of the analyses under hogging moment (negative bending moment and slab in tension) indicate that both the column and the composite beam remained in the elastic range for both the different plates. The pronounced curved shapes of the plates show that

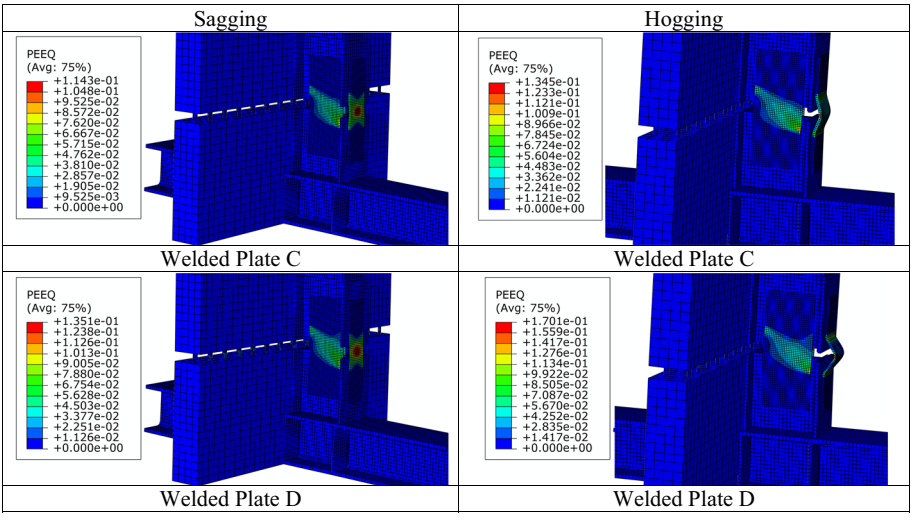

Fig. 7 PEEQ contour plot at sagging (*left*) and hogging (*right*) moment (approximate device rotation = 40 mrad) for the 3D FE models with welded fuses (*plates C* and *D*)

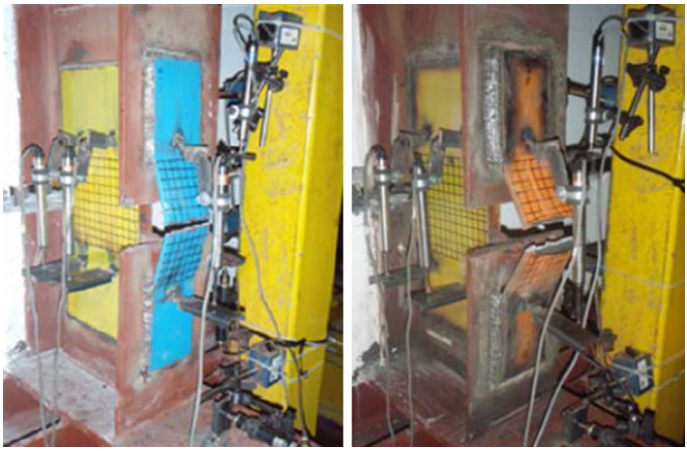

Fig. 8 Typical failure modes of welded flange plates observed in the experimental tests performed at Instituto Superior Tècnico of Lisbon

the attempt of modelling the buckling behavior of the plates is achieved successfully. It is apparent that the resistance in the hogging configuration is controlled by buckling, which occurs in function of both the geometric properties of the flange plates and the free buckling length of the fuse. Numerical results show that the resistance of the fuse under hogging moment is more sensitive to variations of the flange plate geometry than under sagging moment. Buckling of the flange plate of the fuse is clearly observed for the model with plate D, whereas buckling of the fuse plate C under hogging rotation is less evident.

Figure 9 shows the deformed shape and the PEEQ contour plot for the models with bolted flange plates C and D under sagging and hogging rotations (approximate device rotation = 40 mrad).

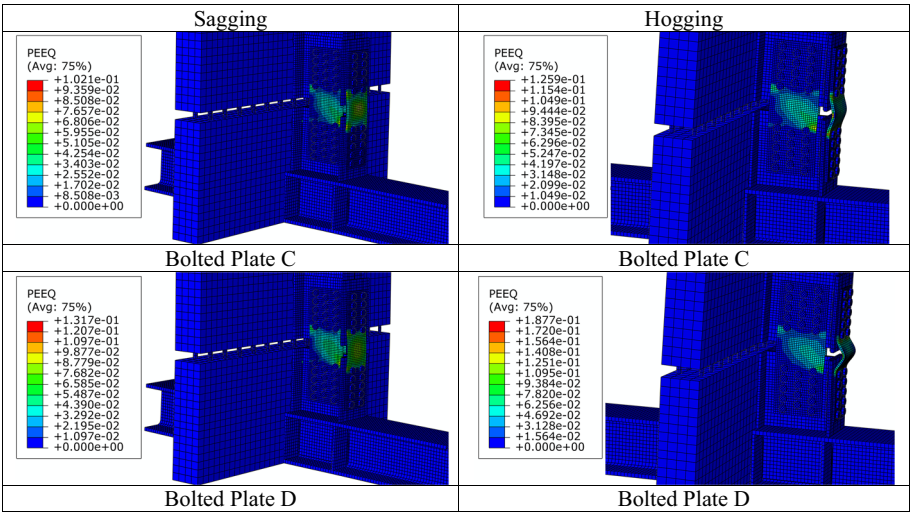

Fig. 9 PEEQ contour plot at sagging (*left*) and hogging (*right*) moment (approximate device rotation = 40 mrad) for the 3D FE models with bolted fuses (*plates C* and *D*)

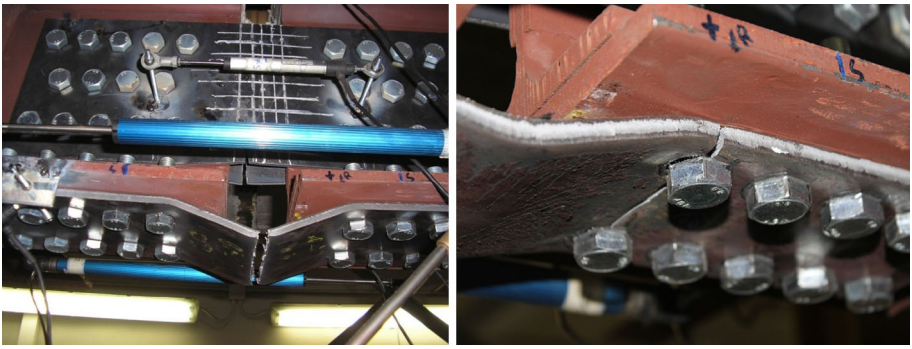

Fig. 10 Typical failure modes of bolted flange plates observed in the experimental tests performed at Politecnico di Milano: failure at the gross section (*left*) and at the net section (*right*)

For sagging rotations, in both the models plastic deformations concentrate in the web and flange plates. However, the analyses indicate that additional reinforcing plates welded to the beam web near the connection are necessary to prevent plastic deformations in the irreplaceable parts of the beam. When sagging and hogging behavior is compared, a significant loss of stiffness, induced by buckling of the fuse plates, occurs under hogging rotation, mainly in the case of plate D. The slippage of bolts contributes to the stiffness degradation of the fuse specimen. The severity of yielding and buckling of the steel plates considerably influence the performance of the fuse device.

Figure 10 shows the two main failure modes of bolted flange plates of the device observed in the experimental tests carried out at Politecnico di Milano within the “Fuseis” project. The fuse devices composed of the thinnest plates were characterized by failures at the gross mid-section of the flange plate after significant strength degradation due to buckling, as a result of hogging bending. In the case of flange plates with increased

thickness, strength degradation due to buckling was not large enough to cause a gross section failure and a failure at the net section of the flange plate was observed due to the lower cross sectional area.

One of the main advantages of the bolted fuse devices is represented by the repairability and replacement of the steel plates. The experimental tests showed that the damaged bolted plates could be changed easily and, during the replacement, the bolt holes did not exhibit any significant damage. In fact, the use of additional reinforcing plates at the web and bottom flange of the fuse parts prevented large deformations of the holes, simplifying the replacement procedures and limiting the slippage of the bolts. In the specimens tested in the laboratory, the cross-sectional areas of the additional reinforcing plates were assumed similar to those of the corresponding parts, web or flanges, of the steel beam. The effectiveness of the repairability of the fuse was also proved through repeated tests on beam-to-column sub-assemblages with plates that were replaced.

Figure 11 compares the numerical monotonic moment-rotation diagrams obtained through the 3D FE models with welded and bolted plate D with the experimental cyclic response obtained with the corresponding test specimens. It can be observed that there is an overall satisfactory agreement between the numerical and experimental results.

In the case of welded fuse, the numerical model is able to predict the experimental behavior with acceptable accuracy, especially in the elastic range. Higher values of the moment capacity are observed in the numerical model, in particular for hogging rotations. It should be considered that in the FE model there is no deterioration from previous cycles that might have induced such a resistance loss during the experimental tests.

In the case of bolted fuse, the numerical model is able to accurately predict the experimental behavior, showing a good fit, especially under the elastic range and hogging rotation. Higher values of the moment resistance are registered in the numerical model under sagging rotation. The slight decrease of elastic stiffness observed for the model with bolted fuses when compared to the one with welded fuses is due to the slippage of the bolts.

Figure 12 shows the numerical monotonic moment-rotation diagrams obtained through the 3D FE models with welded and bolted plate C and the comparison with the experimental cyclic response derived from the corresponding test specimens.

In the case of welded fuse, the yield properties of the numerical model for both hogging and sagging rotations are in a good agreement with the experimental results. The experimental values of the moment capacity under hogging and sagging rotations are accurately predicted by the numerical model.

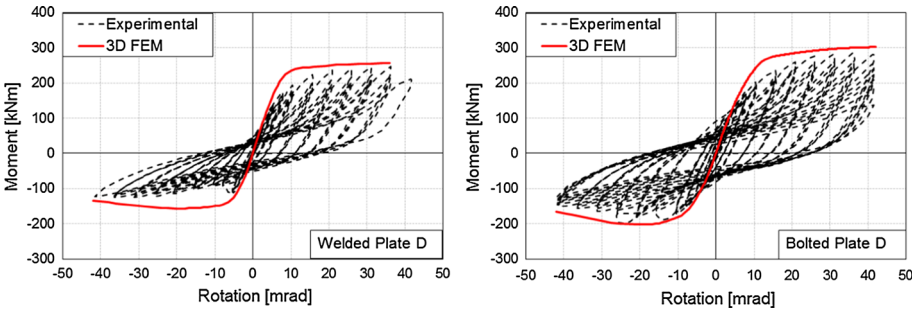

Fig. 11 Moment-rotation diagrams for specimens with plate D (welded fuse and bolted fuse): comparison between 3D FE models and experimental tests

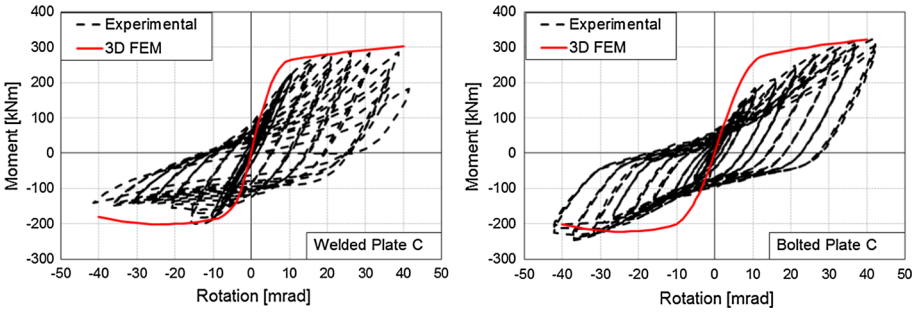

Fig. 12 Moment-rotation diagrams for specimens with plate C (welded fuse and bolted fuse): comparison between 3D FE models and experimental tests

As regards the bolted fuse, it can be noted that the FE model presents higher stiffness than the experimental specimen. It is worth mentioning that this poor agreement is more evident for plate C, which was experimentally tested later, than for plate D. Such a difference could be a consequence of the elastic stiffness loss exhibited by the experimental specimen with plate C due to the damage accumulation in the irreplaceable parts induced by previous tests and low cycle fatigue effects.

Based on the results obtained from both experimental tests and numerical simulations performed on detailed 3D FE models of beam-to-column sub-assemblages, the following observations can be made.

- The dissipative fuses present simple details which facilitate their fabrication, installation and removal. In particular, in the case of bolted fuses the presence of bolts simplifies the removal and replacement of the steel plates.
- The global behavior of the bolted and welded fuses is similar. The response is characterized by high energy dissipation capacity achieved through yielding and buckling of the fuse plates.
- The two types of devices are able to protect beam and column from damage, concentrating inelastic deformations only in the fuses. However, the presence of reinforcing plates welded to the beam web and flange near the connection is necessary to avoid the spreading of inelastic deformation in the adjacent irreplaceable parts of the beams. Such additional plates are recommended mainly in the case of bolted fuses, because they may prevent large plastic deformations that might develop at the holes, simplifying the replacement procedures and limiting slippage of the bolts.
- The failure modes of the two types of devices are similar and consist of the development of cracks at the mid-section of the flange plates, as shown in Fig. 13.
- Experimental and numerical results show that bolted fuses are able of achieving higher moment resistance than welded fuses despite the same net cross-section. Welded fuses present slightly higher elastic stiffness than bolted fuses. Welded fuses reach their yield moments for both sagging and hogging at lower rotations, when compared with bolted fuses. The lower stiffness of bolted fuses is a consequence of the slippage of the bolts inside the holes. Bolted fuses are able of dissipating larger amounts of plastic energy than welded fuses. Steel plates are connected to the beam in the fuse parts by means of high strength friction grip bolts. The energy dissipation capacity of the bolted fuse devices depends on yielding and buckling of the steel plates, but also on friction between the steel plates at the bolted connection interface.

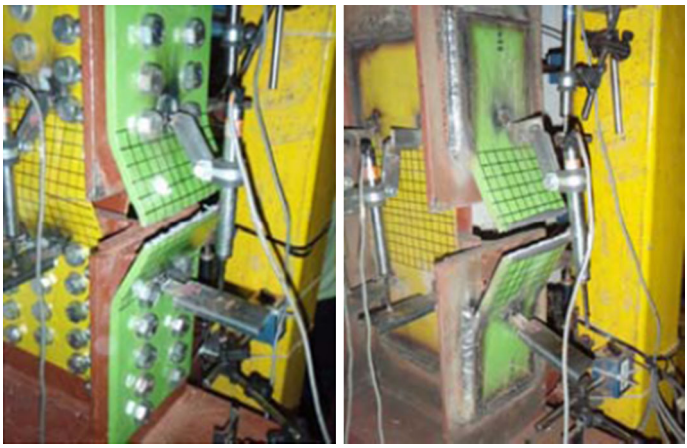

Fig. 13 Comparison between typical failure modes for bolted and welded fuses observed at Instituto Superior Tècnico of Lisbon

3 Simplified numerical model and calibration

In order to extend the results of the numerical analyses carried out on the test specimens to multi-storey frames and to study the behavior of the fuses under seismic excitations, non-linear dynamic analyses were performed on moment resisting composite steel frames with fuse devices. To this aim, the calibration of the models was carried out considering the specimens with plates D, which were the first specimens to be experimentally tested and consequently were not affected by plastic accumulation and damage from previous tests.

3.1 Numerical model

Simplified numerical models of the beam-to-column sub-assemblages tested at Instituto Superior Tècnico of Lisbon were developed by using the computer code SAP2000 (SAP2000). The numerical models were used to further investigate the effects of the application of the fuse devices on the seismic response of different multi-storey composite steel frames. The models consisted of a composite steel beam, equipped with fuse devices, connected to a column with the same geometry used in the experimental test set-up. The potential non-linear behavior of the beam was simulated with a lumped plasticity approach by defining a non-linear plastic hinge at the beam end connected to the column. The fuses were modeled as non-linear link elements with a length equal to the free buckling length of the device. The link element is a non-linear spring with six independent internal deformations for which a non-linear generalized force–deformation relationship can be defined. The multi-linear plastic pivot model was used as hysteresis rule including asymmetrical cross-section behavior with pinching and strength degradation. The link behavior was defined by a moment-rotation curve characterized by different positive and negative moment capacities and initial stiffness of the fuse device. The non-linear behavior was assigned only to the rotational degree of freedom of the link with respect to the major axis of inertia. The constitutive law adopted for the non-linear link was able to represent the dissipated energy, the stiffness and the maximum moment of the fuse during the cyclic loading history. The initial input parameters of the monotonic moment-rotation diagram of

the fuses were obtained from simplified analytical models. The computations of the resistance and stiffness values for all fuses were based on the material properties measured during the experimental campaign. Then, the models were calibrated and refined by using the results of the experimental tests on the specimen sub-assemblages.

3.2 Calibration of the fuses

Figure 14 shows the comparison of the numerical and experimental moment-rotation diagrams of the welded and bolted fuses with plate D. The simplified models are able to accurately capture the non-linear behavior of the devices in terms of stiffness, resistance, ductility and energy dissipation capacity. The moment-rotation diagrams indicate that the hysteretic behavior of the fuses is overall stable and dissipative. It is also characterized by pinching effects due to slippage of the bolts (for bolted fuses) and to buckling of the fuse plates when under hogging rotation. The asymmetry of the diagram in terms of bending moment is due to the presence of the concrete slab and to the strength loss caused by buckling of the fuse plates.

Figure 15 shows the comparison of the moment-rotation diagrams of welded and bolted fuses with different plates obtained by the simplified models. Numerical results clearly show the different behavior between plates with extreme values of the resistance capacity ratio (plate D and plates B-C, respectively), mainly due to the pinching phenomenon and to the differences in strength, which directly affect the energy dissipation capacity. Flange plates D prove to be more sensitive to buckling under hogging rotation due to their geometry (mainly the small thickness), showing more marked pinching effects. Flange plates B and C exhibit higher values of moment capacity than plates D because of their large resistant sections. The curves indicate high energy dissipation capacity for the models with plate C due to stable hysteresis loops.

After the calibration of the numerical models of the welded and bolted fuses with plate D tested at Instituto Superior Tècnico of Lisbon, other moment-rotation curves were created for welded and bolted fuses with different geometrical and mechanical charac-teristics. The input parameters of the monotonic moment-rotation curves of the other two welded and bolted fuses, hereafter denoted as plates PW2 and PB2, were obtained from the 3D FE models. The main geometrical characteristics assumed for the flange plate of the 3D FE model with welded fuse PW2 were: thickness = 14 mm, width = 130 mm, geometric slenderness = 12.1. The 3D FE model with bolted fuse PB2 presented a flange plate with thickness = 14 mm, width = 170 mm, geometric slenderness = 12.1. The initial

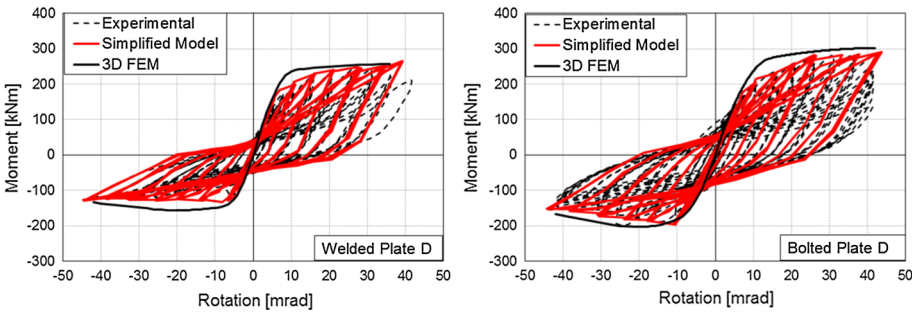

Fig. 14 Moment-rotation diagrams for the specimens with welded and bolted plate D: simplified models versus experimental tests and 3D FE models

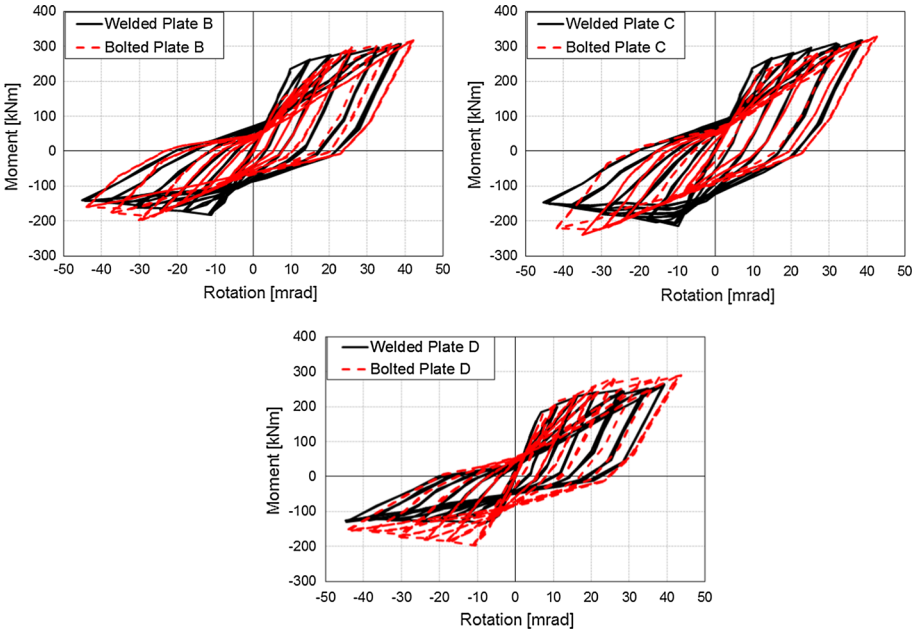

Fig. 15 Moment-rotation diagrams obtained through simplified models with different plates: comparison between welded and bolted fuses

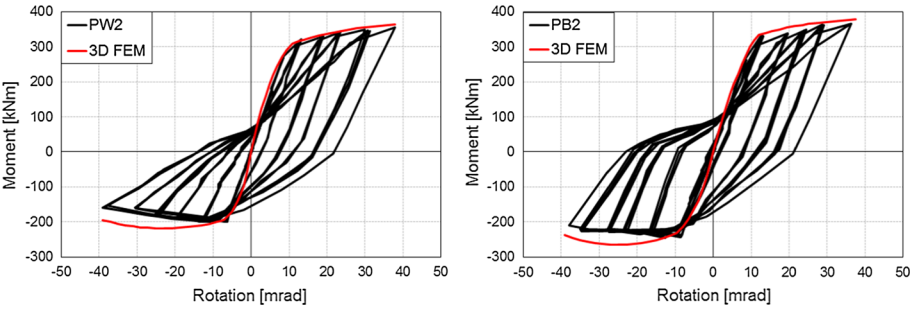

Fig. 16 Moment-rotation diagrams obtained for plate PW2 and plate PB2 through simplified models: comparison with 3D FE models

mechanical characteristics of such new fuses were not affected by the deterioration of the specimen sub-assemblages observed during the experimental tests. The numerical moment-rotation diagrams obtained for the welded (PW2) and bolted (PB2) fuses and the comparison with the monotonic curves derived from the 3D FE models are shown in Fig. 16.

Figure 17 shows the moment-rotation diagrams used for welded (PW1 and PW2) and bolted (PB1 and PB2) plates in non-linear dynamic analyses of composite steel frames in this study. Plates PW1 and PB1 present the same hysteretic behavior as the plates D used in the experimental tests. It is worth mentioning that specimens with plate D were not affected by damage accumulation effects in the irreplaceable parts induced by the previous

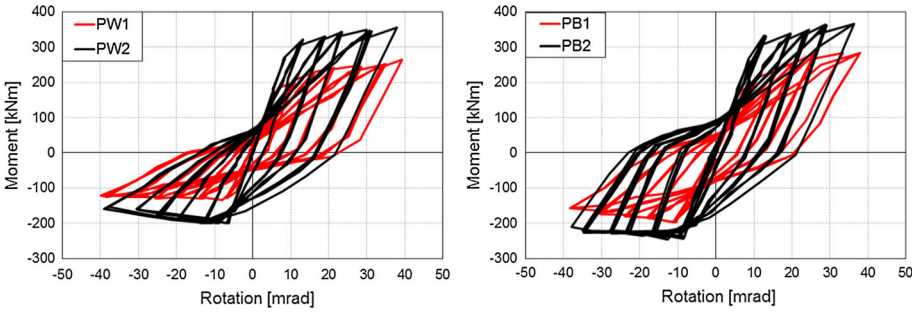

Fig. 17 Moment-rotation diagrams of welded plates (PW1 and PW2) and bolted plates (PB1 and PB2) used in non-linear dynamic analyses of composite steel frames

tests of the experimental campaign. In the case of plates PW1 and PB1, it is clear that buckling of the flange plate under hogging rotation governs the hysteretic behavior of the fuse. In fact buckling causes a marked strength loss under hogging moment, which does not allow the plates to exploit their full bending moment capacity and reduces the energy dissipation capacity. Fuses PB2 and PW2 represent the devices with the highest mechanical characteristics. In particular, the fuse PB2 presents the highest resistance capacity ratio for sagging and hogging rotations and the highest energy dissipation capacity. The fuse PW2 exhibits the highest value of elastic stiffness for sagging and hogging rotations.

4 Steel frame under study

4.1 Numerical model

A multi-storey steel frame with composite beams was analyzed in this study in order to understand and compare the main effects of the application of the different fuse devices. To this aim, the seismic response of the frame with and without fuse devices was evaluated and a comparison of the seismic performance of the innovative seismic resistant steel frames with different fuse plates was carried out.

The frame under study was extracted from a five-storey composite steel building, which was designed according to Eurocode 3, 4 and 8 (EN 1993; EN 1994; EN 1998). The building presents a rectangular plan (21 m × 24 m) with three and four bays in the two orthogonal directions: the four bays of the long side have a span of 6 m and the three bays of the short side have a span of 7 m, as shown in Fig. 18. The building exhibits a storey height equal to 3.5 m. The steel grade used for all the structural members is S355. Dead loads are equal to about 4.5 kN/m^2 and consist of the weights of structural components and partitions; live loads are assumed to be equal to 2 kN/m^2 for all the storeys. Storey masses include dead loads and a percentage of live loads (30 % according to Eurocode 8 for common residential and office buildings). The beams are composite sections consisting of IPE360 steel profile and 12 cm thick reinforced concrete slab, while the columns are made of HEA450 wide flange sections. The geometric dimensions and section profiles of the plane frame under study are illustrated in Fig. 18.

Numerical models of both the conventional steel frame without fuse devices and innovative seismic resistant steel frames with different fuse devices were developed using

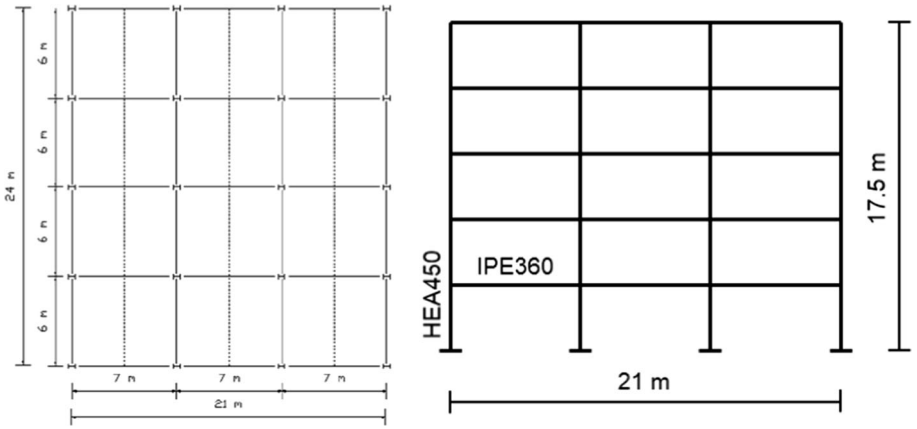

Fig. 18 Plan of the building and composite steel frame under study

the computer code SAP2000. Hereafter, the conventional frame is denoted as "F1" and the innovative seismic resistant frames are denoted as "FPij", where i and j indicate, respectively, the type of fuse (W = welded or B = bolted) and the flange plate (1 or 2) used in the model.

A lumped plasticity modeling approach was employed for the non-linear models of the frames. Beam and column elements were modeled as frame elements and non-linearity was concentrated in plastic hinges at their ends. To characterize the non-linear behavior of a plastic hinge, the generalized force–deformation properties suggested in FEMA 356 (FEMA 356, 2000) were implemented. For the beams flexural moment hinges were considered, while plastic hinges accounting for the interaction between axial force and bending moment were defined for the columns. Beam-to-column joints were considered as rigid in accordance with the connection detailing of the experimental tests.

The models of the different fuse devices were implemented in the numerical models of the frames. The length of the beams was subdivided into different elements in order to take into account both the presence of the fuse devices and the part of the beam reinforced with additional welded plates. The fuses were modeled as non-linear link elements inserted in the beams with a length equal to the free buckling length of the welded plates. The fuse devices were placed at a distance equal to the beam depth from the beam-to-column connections. The multi-linear plastic pivot model was used as hysteresis rule for the fuses. The values of the parameters used for the hysteretic model were those obtained from the calibration of the models of the specimens tested at Instituto Superior Tècnico of Lisbon.

The part of the beam reinforced with additional welded plates, aimed at avoiding spreading of plasticity to the connection, was reproduced in the numerical models by using different cross-sections and plastic hinges properties around the device. The length of these regions was assumed in the model in accordance with the geometry of the experimental specimens.

Figure 19 shows the resistance capacity ratio and the elastic stiffness under sagging and hogging rotations for both welded and bolted fuses with different flange plates. The fundamental vibration periods of the frames under study are reported in Table 2.

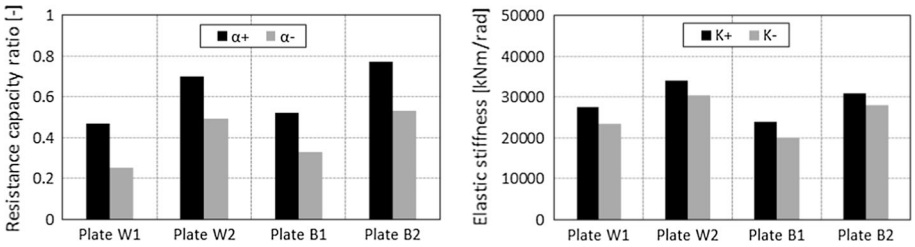

Fig. 19 Resistance capacity ratio (*left*) and elastic stiffness (*right*) under sagging and hogging rotations for both welded and bolted fuses with different flange plates

Table 2 Fundamental vibration periods [s] of the frames under study

F1	FPW1	FPB1	FPW2	FPB2
1.067	1.179	1.201	1.147	1.165

Fig. 20 Response spectra of the artificial accelerograms

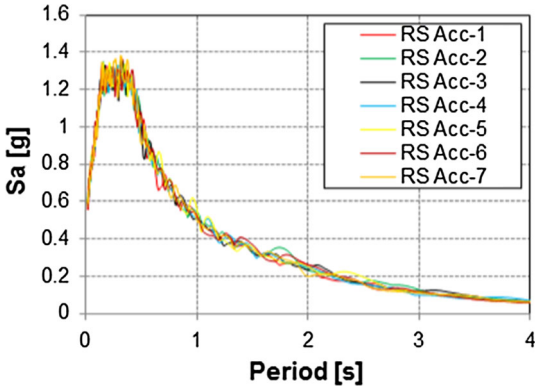

4.2 Non-linear dynamic analyses

The seismic performance of the frames under study was assessed through non-linear dynamic analyses with response spectrum-compatible artificial accelerograms. The set of artificial ground motions consisted of seven different records that were generated so as to match the Eurocode 8 response spectrum (Type 1, soil type A, 5 % viscous damping) using the computer code SIMQKE (Vanmarcke et al. 1976). The response spectra of the artificial accelerograms used in this study are shown in Fig. 20. The non-linear dynamic analyses were performed for three different peak ground accelerations (PGA) of the artificial earthquake records, ranging between 0.3 and 0.7 g.

The results of the non-linear dynamic analyses are presented using the average values of the results obtained using the seven artificial records. The maximum top displacements of the different frames are shown in Fig. 21 for three different peak ground accelerations.

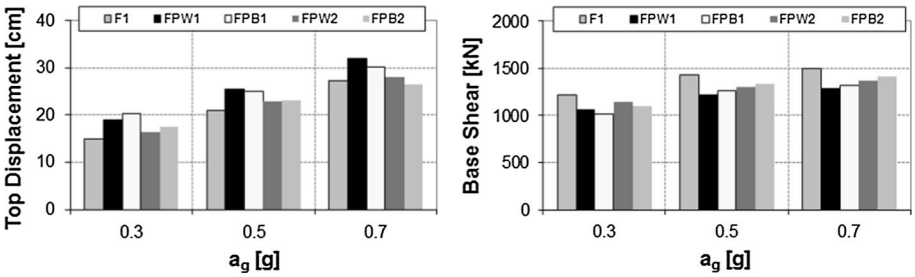

Fig. 21 Maximum values of top displacement and base shear of the frames under study for different peak ground accelerations

The maximum top displacements of the innovative frames with fuses are generally larger than those registered for the conventional frame, because the insertion of the fuse devices has the consequence of reducing the lateral stiffness of the frames.

Comparing the seismic performance of the different innovative frames, it can be argued that the initial stiffness and moment resistance adopted for the constitutive laws of the fuse devices affect the results. In the case of PGA = 0.3 g, the innovative frame FPW2 experiences smaller top displacement than the other innovative frames (the moment-rotation curve adopted for the fuse plate PW2 presents higher elastic stiffness than the other fuses). In the case of PGA = 0.7 g, smaller top displacements are registered for frame FPB2 (the moment-rotation curve adopted for the fuse plates PB2 presents higher moment resistance than the other fuses). Moreover, the conventional frame F1 and the innovative frame FPB2 show similar values of top displacements. Numerical results highlight that a significant reduction of the mechanical characteristics of the fuse (initial stiffness and moment resistance) can be detrimental to the seismic performance of the innovative frames in terms of top displacements, as observed for frames FPB1 and FPW1.

Figure 21 shows the maximum values of the base shear of the frames for different peak ground accelerations. The maximum values of the base shear of the innovative frames with fuses are always smaller than the conventional frame. The decrease of the base shear of the innovative frames depends mainly on the resistance capacity ratio of the fuse devices. Frames FPB2 and FPW2 exhibit higher values of the base shear than frames FPB1 and FPW1, because they are equipped with fuses characterized by high values of moment resistance.

Figure 22 compares the amount of plastic energy dissipated in conventional and innovative frames with different plates under PGA = 0.7 g. The plastic energy dissipated in columns, beams and fuses is reported for the different frames. The results demonstrate the beneficial effect of the presence of the fuses on the overall energy dissipation capacity of the frame. As can be noted, the total amount of hysteretic energy dissipated in innovative frames with fuses is higher than in conventional frame. This result can be explained by the higher values of plastic energy dissipated by fuses in innovative frames than by beams in conventional frame.

The increase of energy dissipation capacity is related to the type of fuse implemented in the model. Frame FPB2 presents the highest value of plastic energy dissipated in fuses, because the fuse PB2 is characterized by a stable hysteretic behavior. On the contrary, frames FPW1 and FPB1 exhibit the smallest amount of plastic energy dissipated in fuses because fuses PW1 and PB1 show stiffness and strength degradation with marked pinching effects, as shown in Fig. 17.

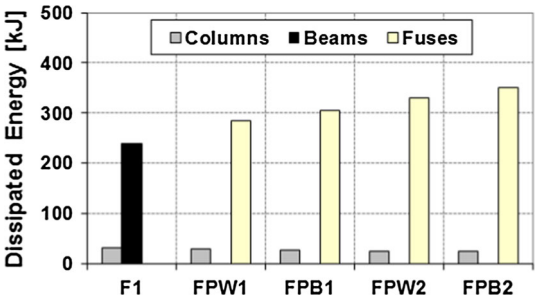

Fig. 22 Plastic energy dissipated in conventional frame (F1) and in innovative frames with different fuses (FP) under PGA = 0.7 g

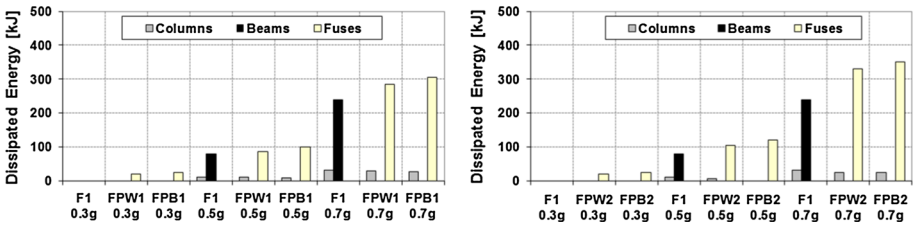

Fig. 23 Plastic energy dissipated in conventional frame (F1) and in innovative frames with different fuses (FP) for different peak ground accelerations

Figure 23 shows the plastic energy dissipated in conventional frame and in innovative frames with fuses for different peak ground accelerations. For smaller values of PGA, the innovative frames dissipate small amounts of plastic energy in fuses, whereas the conventional frame practically remains in the elastic range. The plastic energy dissipated in innovative frames is similar for all the plates used in the models. Innovative frames FPW1 and FPB1 yield early due to the low stiffness and strength of the fuses and start dissipating plastic energy earlier than innovative frames FPW2 and FPB2. For each level of PGA, the amount of energy dissipated by the fuse PB2 is larger than that dissipated by the fuse PW2.

The number and distribution of plastic hinges are very similar for the different frames at the end of the non-linear dynamic analyses. In conventional frame plastic deformations occur at the beam ends and at the base of the ground level columns, reflecting the design of the frame according to the provisions of Eurocode 8. In innovative frames plastic deformations concentrate in the fuses and the beam ends are protected remaining in the elastic range. The fuses act as dissipative devices, thus avoiding the formation of plastic deformations into the columns, except at the base of the ground level columns, and minimizing the repair costs even though the initial costs of construction may be higher than those for conventional frames. Moreover, numerical results show that no soft story mechanism appears for all the examined frames when subjected to severe seismic excitations with PGA = 0.7 g.

Figure 24 indicates the maximum values of rotations computed in beams and fuses of the first storeys for the different frames under study when subjected to seismic excitation with PGA = 0.7 g. As can be noted, the maximum rotations registered in fuses of inno-vative seismic resistant frames are larger than those in beams of the conventional frame. In particular, considerable rotations develop in fuses of frames FPB1 and FPW1 during seismic excitation. However, the experimental tests have shown that such rotations can be accommodated by the devices. The maximum values of the rotations attained by the fuses

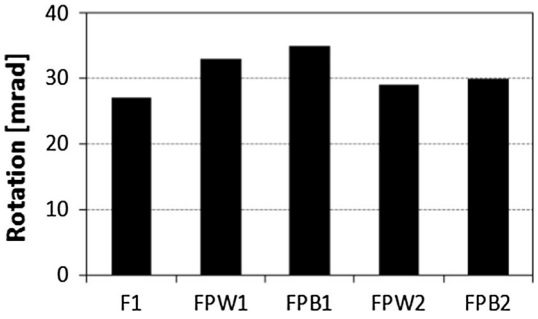

Fig. 24 Maximum rotation in beams (for frame F1) and fuses (for innovative frames FP) under PGA = 0.7 g

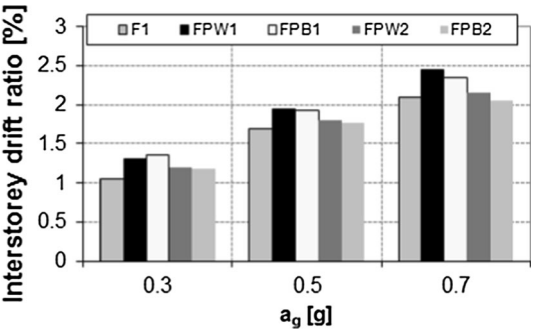

Fig. 25 Maximum interstorey drift ratio of the conventional frame (F1) and innovative frames with different fuses (FP) for different peak ground accelerations

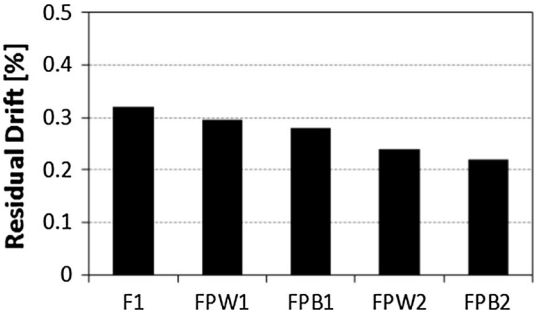

Fig. 26 Residual drift ratio of the conventional (F1) and innovative (FP) frames under PGA = 0.7 g

of the frames in non-linear dynamic analyses were about 35 mrad, that is a value for which the fuses of the experimental tests showed stable hysteresis loops and high energy dissipation capacity.

Figure 25 shows the maximum interstorey drift ratio (IDR) of the conventional and innovative frames for different peak ground accelerations. The maximum IDR values of the innovative frames with fuses are generally larger than those observed for the conventional frame: the maximum IDR values are registered for frames FPW1 and FPB1. It can be noted that innovative frame FPB2 and conventional frame F1 exhibit similar IDR values, mainly under strong seismic excitations.

Under severe earthquakes structures may exhibit large residual drifts that may induce problems in the post-earthquake use and high repair costs. The residual drift ratio is computed for all the frames under study at the end of the non-linear dynamic analyses and

the results obtained under PGA = 0.7 g are reported in Fig. 26. It can be noted that the values of the residual drift ratio are lower than the limit of 0.5 % for all the frames. Numerical results show a decrease of the residual drift ratio with the increase of the mechanical characteristics of the fuses. The innovative frame FPB2 experiences smaller residual drifts than the other frames, thus allowing for an easy repair after the earthquake. Limited values of residual drifts are beneficial mainly for frames with bolted devices, because after severe earthquakes, in the presence of excessive residual plastic deformations, bolted fuses are more difficult to replace than welded fuses.

4.3 Overall ductility factor and collapse mechanisms

Non-linear static (pushover) analyses were performed in order to estimate the overall ductility factor, the damage distribution and the expected plastic collapse mechanism of the different frames. Numerical results confirm the reduction of the lateral stiffness of the innovative frames with fuses when compared with the conventional frame.

The overall ductility factor μ is computed for all the frames in order to evaluate the plastic displacement capacity that innovative frames with fuses can provide till the achievement of the plastic mechanism. The ductility factor μ is defined as the ratio between the roof dis-placement δ_u when plastic hinges form in a number of sections sufficient for the development of overall structural instability and the roof displacement δ_y associated with the formation of the first plastic hinge. Figure 27 shows the overall ductility factors obtained for conventional (F1) and innovative (FP) frames. The conventional frame F1 exhibits smaller values of the overall ductility factor than innovative frames with fuses, except the case of the innovative frame FPW1. The maximum value of the overall ductility factor is registered for the inno-vative frame FPB2, which presents the highest resistance capacity ratio of the fuse. The use of higher resistance capacity ratios of the bolted fuse generates higher values of base shear in the capacity curve and the collapse mechanism is deferred.

The collapse mechanisms obtained from pushover analyses are similar for conventional frame and innovative frames with dissipative fuses. A global collapse mechanism involving beams (beams ends for conventional frame and fuses for innovative frames) and the bases of the ground level columns is registered for both the two types of frames. Nevertheless, in conventional frame some plastic hinges are observed in the columns of different storeys. On the contrary, in innovative frames with dissipative fuses plastic hinges are located only in the fuses and at the bases of the ground level columns. Consequently, innovative frames with fuse devices can ensure a better control of plastic mechanism than conventional frame under high horizontal loads. The same collapse mechanism is registered for all the innovative frames.

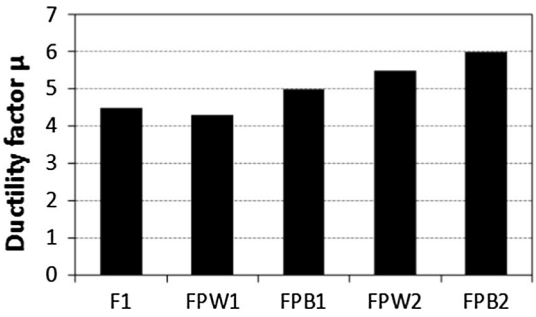

Fig. 27 Values of the overall ductility factor for conventional (F1) and innovative (FP) frames

5 Extension to three-dimensional structures

5.1 Buildings under study

The numerical results obtained on a plane steel frame were extended to the case of three-dimensional steel building structures with composite beams. The seismic response of three buildings with different number of storeys was analyzed in this study. All the buildings exhibit a square plan (15 m x 15 m) with three bays for each side (bay width equal to 5 m) and present an interstorey height equal to 3.5 m. The first building structure, denoted as S1–3, is 10.5 m high and consists of three storeys; the second building structure, denoted as S1–6, is 21 m high and consists of six storeys; the third building structure, denoted as S1–9, is 31.5 m high and consists of nine storeys.

Structural steel S275 is used for all the structural elements of the three buildings. All the columns of the investigated buildings are composed by means of two hot-rolled double T profiles welded along the longitudinal axis to form an X-shaped section. The dimensions of the column sections change in function of the number of the storeys of the building. All the beam-to-column connections are moment resistant. The beam sections are the same used in the beam-to-column sub-assemblages of the experimental tests.

The gravity loads consist of dead loads and live loads: dead loads are equal to about 4 kN/m^2 and live loads are assumed equal to 2 kN/m^2, which is a typical value for an office or residential building. Storey masses include dead loads and a percentage of live loads (30 % according to Eurocode 8 for common residential and office buildings). Flexural moment hinges are adopted for beams, while PMM (axial force biaxial moment) hinges are defined for columns and the properties are calculated according to FEMA 356 (FEMA 356, 2000).

Innovative seismic resistant steel buildings with fuse devices were also created. They are denoted as "SPij-n", where ij and n indicate the plate type used in the model and the number of the storeys of the building, respectively. The models of the different fuse devices were implemented in the numerical models of the frames. The values of the parameters used for the hysteretic models of the fuses are those obtained from the calibration of the models of the specimens tested at Instituto Superior Tècnico of Lisbon.

The elevations and the three-dimensional views of the three buildings under study, along with the column and beam cross-sections, are shown in Fig. 28. The fundamental vibration periods of the different buildings, with and without fuse devices, are compared in Fig. 29.

5.2 Non-linear dynamic analyses

The seismic performance of the buildings under study was assessed through non-linear bidirectional dynamic analyses. The set of artificial accelerograms consisted of three couples of different records that were generated so as to match the Eurocode 8 response spectrum (Type 1, soil type A, 5 % viscous damping) using the computer code SIMQKE (Vanmarcke et al. 1976). Figure 30 shows the response spectra of the artificial accelerograms used for the two orthogonal directions in this study. The non-linear bidirectional dynamic analyses were performed for different peak ground accelerations (PGA) of the artificial earthquake records, ranging between 0.3 and 0.7 g.

Figure 31 shows the maximum top displacements of the buildings under study in the two orthogonal directions for three different peak ground accelerations. In the case of

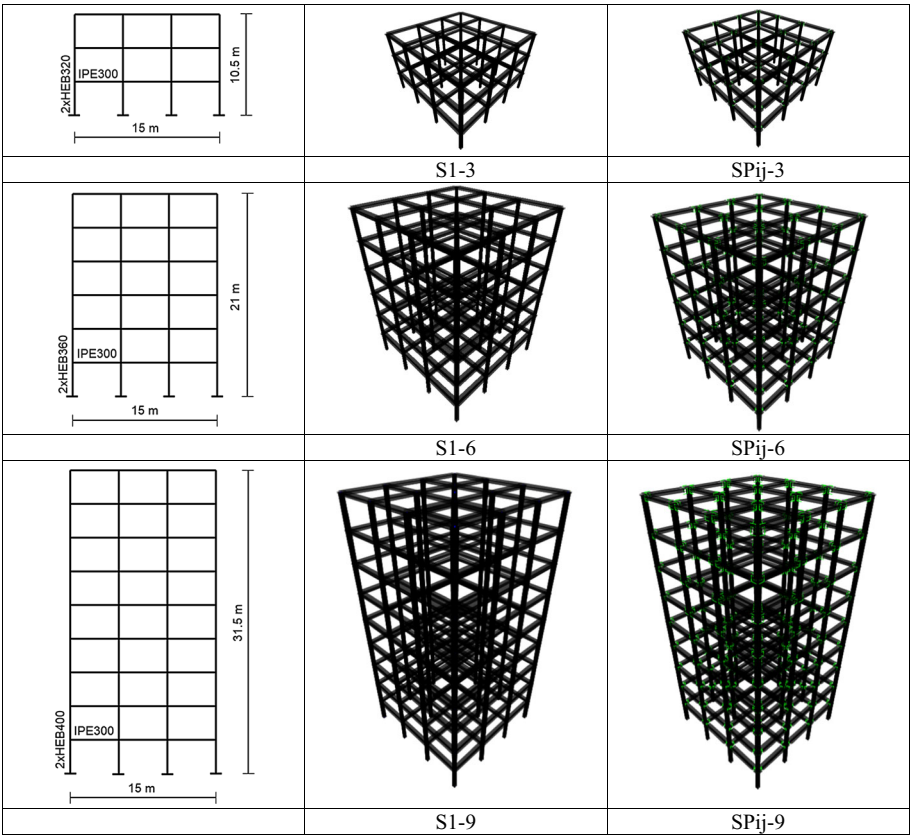

Fig. 28 Three-dimensional building structures under study: conventional (S1) and innovative (SP) buildings

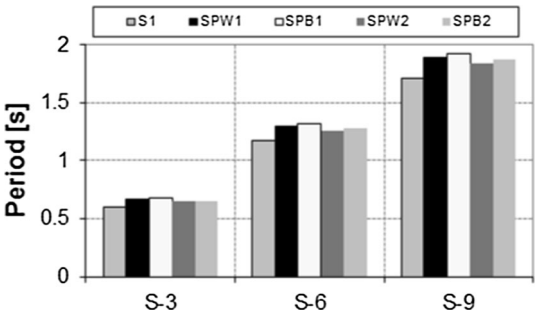

Fig. 29 Fundamental vibration periods of the buildings under study

PGA = 0.3 g, buildings SPW2 generally exhibit smaller top displacements because of the high values of the elastic stiffness adopted for the fuse plate PW2. In the case of PGA = 0.7 g, smaller top displacements are registered for buildings SPB2 because the fuse plate PB2 presents high values of moment resistance and large dissipation capacity; moreover, the innovative buildings SPB2 and the conventional buildings S1 show similar

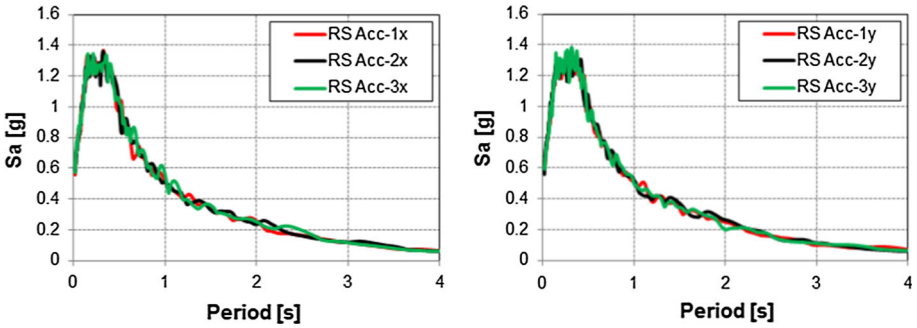

Fig. 30 Response spectra of the artificial accelerograms for non-linear bidirectional dynamic analyses (*x* and *y* directions)

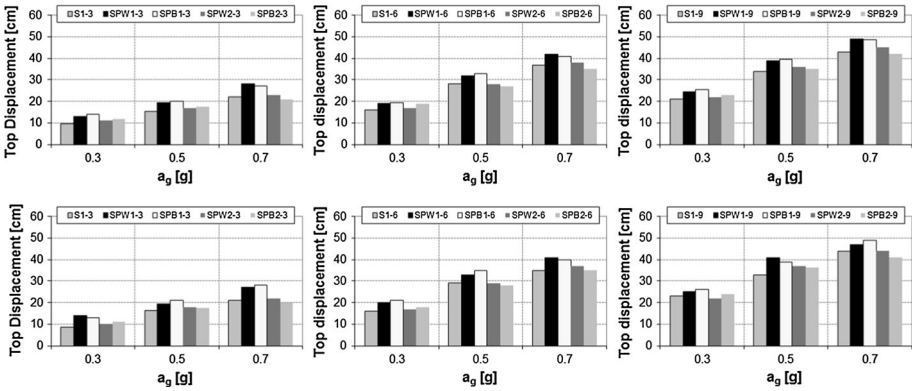

Fig. 31 Maximum top displacement of the buildings under study for different peak ground accelerations: x (*top*) and y (*bottom*) directions

values of top displacements for all the building heights. The innovative buildings SPW1 and SPB1 present significant increases of top displacements when compared with buildings SPB2, mainly for high values of seismic intensity levels, due to their small energy dissipation capacity. Similar results can be observed for all the buildings with different number of storeys.

Figure 32 shows the amount of plastic energy dissipated in conventional buildings and in innovative buildings with fuses under PGA = 0.7 g. Numerical results confirm that buildings with bolted fuses exhibit higher energy dissipation capacity when compared with corresponding buildings with welded fuses as well as with conventional buildings. The plastic energy dissipated by bolted fuses is generally larger than the one dissipated by

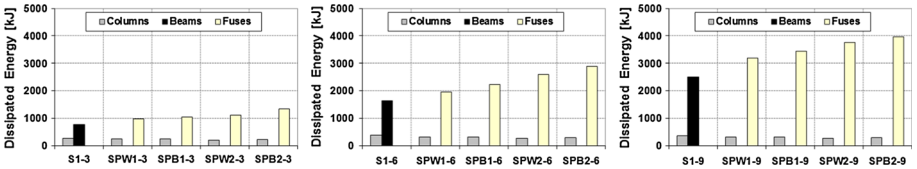

Fig. 32 Plastic energy dissipated in conventional (S1) and innovative (SP) buildings under PGA = 0.7 g

welded fuses. The overall energy dissipation capacity of building SPB2 is larger than the one of all the other buildings.

6 Conclusions

The seismic performance of two types (welded and bolted) of fuse devices for earthquake resistant composite steel frames is investigated and compared through experimental tests and numerical analyses. The device is made by introducing a discontinuity on the composite beam of a frame and assembling the two parts of the beam through steel plates that can be welded or bolted to the beam web and flange.

From an overall analysis of the results obtained in this study, the following remarks can be made on the seismic behavior of the two types of fuses.

- The global behavior of the two types of fuses is similar and it is characterized by high energy dissipation capacity achieved through yielding of the steel plates. Both the two types of fuse devices are able to protect both the beam and the column from damage.
- The failure modes of the two types of devices are similar and consist of the development of cracks at the mid-section of the flange plates. In the case of bolted flange plates with increased thickness, strength degradation due to buckling is not large enough to cause a failure at the gross mid-section and a failure at the net section is observed due to the smaller cross sectional area.
- Experimental and numerical results show that bolted fuses are able of achieving higher moment resistance than welded fuses despite the same net cross-section. On the contrary, welded fuses present higher elastic stiffness than bolted fuses and reach their yield moments for both sagging and hogging at lower rotations. The lower stiffness of bolted fuses is a consequence of the slippage of the bolts inside the holes. Bolted fuses are able of dissipating larger amounts of plastic energy than welded fuses.
- Bolted fuses can be replaced more easily than welded fuses, avoiding the cumbersome work of welding and unwelding the fuse plates. However, it is worth mentioning that bolted fuses may be more difficult to replace than welded fuses when the structure experiences severe damage with excessive residual plastic deformations after strong earthquakes. The use of additional reinforcing plates welded to the web and to the bottom flange of the steel beam near the fuse may prevent large deformations of the holes, simplifying the replacement procedures and limiting the slippage of the bolts.

As regards the effects of the different fuses on the seismic performance of composite steel structures, the following conclusions can be made.

- Both the typologies of devices are able to concentrate plastic deformations in repairable fuses, which not only prevent collapse under severe earthquakes, but also limit structural damage and allow for repairability and replacement after moderate-to-severe earthquakes when residual plastic deformations are not excessive.
- Innovative frames generally exhibit larger values of top displacements than conventional frames. In the case of lower values of PGA, smaller top displacements are generally registered for frames with welded fuses that present higher stiffness than bolted fuses. For high values of PGA, frames with bolted fuses experience smaller top displacements than frames with welded fuses because bolted fuses present higher energy dissipation capacity and higher moment resistance than welded fuses. Moreover, the top displacements observed for frames with bolted plates PB2 are

comparable or smaller than those registered for conventional frames under severe earthquakes. Innovative frames with bolted fuses undergo limited values of residual drifts, thus reducing the problems related to the replacement of the bolted plates.

- The global energy dissipation capacity of innovative frames is larger than conventional frames due to the presence of the fuse devices. For innovative frames the increase of the energy dissipation capacity depends on the characteristics of the fuse devices. Frames with bolted fuses dissipate larger amounts of plastic energy than frames with welded fuses. This result can be explained by the higher values of hysteretic energy dissipated by bolted fuses than by welded fuses. Innovative frames with bolted fuses start dissipating plastic energy earlier than innovative frames with welded fuses.
- The collapse mechanism of the innovative frames with both the typologies of devices is ductile involving all the fuses and the bases of the ground level columns. Damage concentrates in fuses that are easily replaceable, thus avoiding the formation of plastic hinges into the columns and minimizing the repair costs, even though the initial costs of construction may be higher than those for conventional frames.
- Innovative frames with fuses exhibit larger values of the overall ductility factor than conventional frames. In particular, innovative frames with bolted fuses present larger values of the overall ductility factor than corresponding innovative frames with welded fuses. The high deformation capacity of both the typologies of fuses is demonstrated by the results of the experimental tests.

In conclusion, the use of bolted fuses is preferred because it allows for higher energy dissipation capacity and easier replacement of the steel plates than welded fuses.

Acknowledgments The studies reported in this paper were conducted within the scope of the FUSEIS (Dissipative Devices for Seismic Resistant Steel Frames, reference RSFR-CT-2008-00032) research project, financed by the Research Fund for Coal and Steel, of the European Commission.

References

ABAQUS Theory Manual, USA, 2014

Calado L, Proenca JM, Espinha M, Castiglioni CA (2013a) Hysteretic behavior of dissipative welded fuses for earthquake resistant composite steel and concrete frames. Steel Compos Struct 14(6):547–569

Calado L, Proenca JM, Espinha M, Castiglioni CA (2013b) Hysteretic behavior of dissipative bolted fuses for earthquake resistant steel frames. J Constr Steel Res 85:151–162

Castiglioni CA, Kanyilmaz A, Calado L (2012) Experimental analysis of seismic resistant composite steel frames with dissipative devices. J Constr Steel Res 76:1–12

Danai D, Dougka G, Vayas I (2015) Seismic behavior of frames with innovative energy dissipation systems (FUSEIS1-2). Eng Struct 90:83–95

Elghazouli AY (2010) Assessment of European seismic design procedures for steel framed structures. Bull Earthq Eng 8(1):65–89

EN 1993 (2004) Eurocode 3: design of steel structures

EN 1994 (2004) Eurocode 4: design of composite steel and concrete structures

EN 1998 (2004) Eurocode 8: design of structures for earthquake resistance

FEMA 356 (2000) Prestandard and commentary for the seismic rehabilitation of buildings

Giannuzzi D, Ballarini R, Hucklebridge A, Pollino M, Valente M (2014) Braced ductile shear panel: new seismic-resistant framing system. J Struct Eng ASCE 140(2):1–11

Mansour N, Christopoulos C, Tremblay R (2011) Experimental validation of replaceable shear links for eccentrically braced steel frames. J Struct Eng ASCE 137(10):1141–1152

SAP2000 Static and dynamic finite element analysis of structures. Computers and Structures Inc., Berkeley

Shen Y, Christopoulos C, Mansour N, Tremblay R (2011) Seismic design and performance of steel moment-resisting frames with nonlinear replaceable links. J Struct Eng ASCE 137(10):1107–1117

Soong TT, Spencer BF Jr (2002) Supplemental energy dissipation: state-of-the-art and state-of-the-practice. Eng Struct 24(3):243–259
Vanmarcke EH, Cornell CA, Gasparini DA, Hou S (1976) SIMQKE: A program for artificial motion generation. Civil Engineering Department, Massachusetts Institute of Technology, Massachusetts
Vasdravellis G, Valente M, Castiglioni CA (2009a) Behavior of exterior partial-strength composite beam-to-column connections: experimental study and numerical simulations. J Constr Steel Res 65(1):23–35
Vasdravellis G, Valente M, Castiglioni CA (2009b) Dynamic response of composite frames with different shear connection degree. J Constr Steel Res 65(10–11):2050–2061